

Gated nonlinear transport in organic polymer field effect transistors

B.H. Hamadani and D. Natelson

*Department of Physics and Astronomy,
Rice University, 6100 Main St., Houston, TX 77005*

(Dated: November 20, 2018)

Abstract

We measure hole transport in poly(3-hexylthiophene) field effect transistors with channel lengths from $3\ \mu\text{m}$ down to 200 nm, from room temperature down to 10 K. Near room temperature effective mobilities inferred from linear regime transconductance are strongly dependent on temperature, gate voltage, and source-drain voltage. As T is reduced below 200 K and at high source-drain bias, we find transport becomes highly nonlinear and is very strongly modulated by the gate. We consider whether this nonlinear transport is contact limited or a bulk process by examining the length dependence of linear conduction to extract contact and channel contributions to the source-drain resistance. The results indicate that these devices are bulk-limited at room temperature, and remain so as the temperature is lowered. The nonlinear conduction is consistent with a model of Poole-Frenkel-like hopping mechanism in the space-charge limited current regime. Further analysis within this model reveals consistency with a strongly energy dependent density of (localized) valence band states, and a crossover from thermally activated to nonthermal hopping below 30 K.

PACS numbers:

I. INTRODUCTION

Electronic devices based on organic semiconductors, such as polymeric field effect transistors (FETs) and light emitting diodes (LEDs), have attracted much interest as possible inexpensive and flexible alternatives to inorganic devices[1, 2]. While there has been considerable improvement in device properties, the detailed mechanism of electronic transport in organic thin film devices remains a subject of active investigation.

Charge motion in undoped organic field effect devices is often characterized in the linear (small source-drain bias) regime by a field-effect mobility. In disordered polymer semiconductors this mobility, μ , is strongly temperature dependent near room temperature, consistent with thermally assisted hopping between localized states dispersed throughout the polymer film[3]. These localized states are likely to be polaronic[4]. Several different models for hopping transport in these materials have been used to interpret experimental data from ~ 200 K to room temperature, including simple thermal activation[5], 2d variable range hopping (VRH)[6], and percolative VRH with an exponential density of states[7]. While some models work better with some specific samples, generally distinguishing between them is difficult.

The situation is complicated by the fact that the effective mobilities inferred in this manner depend on T , gated charge density[8], source-drain bias, and contact effects. Parasitic contact resistances in particular can be important. Experiments in several organic semiconductor/electrode combinations[9, 10, 11, 12, 13, 14, 15, 16] have shown that contact resistances can be a significant fraction of the total source-drain resistance in the linear regime in short devices. Data in this shallow channel limit must be corrected accordingly for this parasitic series resistance, R_s , to find the true mobility within the semiconductor. As with μ , one must bear in mind that R_s typically depends on temperature, gate voltage, and local electric field[12]. When examining transport properties of organic FETs, it is therefore important to determine whether the devices are dominated by the bulk (channel) or the contacts.

We report *nonlinear* transport measurements in field-effect devices made from high quality, solution cast, regio-regular poly(3-hexylthiophene) (P3HT), with channel lengths from $3\ \mu\text{m}$ to $200\ \text{nm}$ and aspect ratios of 10. Higher temperature properties at low source-drain fields are consistent with those observed by other investigators. From $200\ \text{K}$ to $10\ \text{K}$, we ob-

serve gate-modulated nonlinear IV characteristics. To understand the effects of contacts in our series of devices, we examined both the devices described above, and an additional series of fixed-width FETs to obtain the channel and contact resistances as a function of temperature. These data demonstrate that (a) the fixed-aspect-ratio devices are bulk (not contact) limited at high temperatures; and (b) the contribution of contacts relative to the channel actually *decreases* as the temperature is lowered, so that bulk-limited devices tend to remain so as T is decreased. Since the nonlinearities in the IV curves become more pronounced at low temperatures and in wider devices (for which contact resistance are proportionately less important), it is unlikely that these nonlinearities are due to contact effects in these geometries. We find that the nonlinear data are consistent with a model of Poole-Frenkel (PF) type conduction in the space-charge limited (SCL) regime. Within this framework, the strong gate and temperature dependence of this conduction are consistent with a density of localized valence states that varies approximately exponentially in energy. Still within this model, at temperatures below 30 K there appears to be a crossover from thermally assisted hopping to a nonthermal mechanism. These nonlinear data over a broad temperature range constrain any other models of transport in such devices. Studying FETs in this nonlinear regime allows comparisons between models not readily performed with linear transport data.

II. EXPERIMENTAL DETAILS

Devices are made in a bottom-contact configuration (see Fig. 1 inset) on a degenerately doped $p+$ silicon wafer to be used as a gate. The gate dielectric is 200 nm of thermal SiO_2 . Source and drain electrodes are patterned using standard electron beam lithography. The electrodes are deposited by electron beam evaporation of 4 nm Ti and 25 nm of Au followed by liftoff. The fixed-aspect-ratio devices have channel lengths ranging from 3 μm down to 200 nm, with the channel width scaled to maintain $w/L = 10$. Larger FET devices ($w = 1$ mm, $L = 50$ μm) are also prepared for comparison. We also examine a second set of devices with fixed width $w = 100$ μm and channel lengths varying from 5 μm up to 40 μm , specifically for probing contact resistance issues.

The organic semiconductor is 98% regio-regular P3HT[17], a well studied material[18, 19, 20]. P3HT is known from x-ray scattering to form nanocrystalline domains with sizes on the order of 20 nm[18, 20], and more ordered films correlate with higher measured mobili-

ties. RR-P3HT is dissolved in chloroform at a 0.02% weight concentration, and is solution cast[18] onto ozone-cleaned, chloroform-swabbed substrates. The fixed-aspect-ratio series of devices are from one casting, while the fixed-width series are from a second casting. The resulting film thicknesses over the channel region are tens of nm as determined by atomic force microscopy (AFM), though casting produces somewhat nonuniform films. All devices are stored in vacuum desiccators until use. The measurements are performed in vacuum ($\sim 10^{-6}$ Torr) in a variable-temperature probe station using a semiconductor parameter analyzer (HP4145B).

III. RESULTS AND DISCUSSION

At room temperature, the devices operate as standard p -type FETs in accumulation mode[6, 18, 19, 20, 21]. With the source electrode as ground, in the linear regime we extract[5] an effective mobility from the transconductance. That is, from data of source-drain current, I_D versus the gate voltage, V_G , at a fixed low drain voltage, V_D , we compute $\mu = (g_m L)/(w C_i V_D)$, where $g_m \equiv \partial I_D / \partial V_G$ is the transconductance, C_i is capacitance per unit area of the gate insulator, and w/L is the aspect ratio. The relevance of parasitic contact resistances will be addressed below. As is reported elsewhere[9], the mobility is gate voltage dependent, increasing with increasing V_G . It also increases with increasing source-drain voltage. Effective mobilities are typically between 10^{-3} and 10^{-2} cm^2/Vs , and apparent threshold voltages (V_T), though not necessarily meaningful[21], are low (< 2 V). For $L = 50$ μm FETs operated in the saturation regime, the on/off ratio is typically ~ 650 , comparing between gate voltages of -95 V and 0 V. As temperature is reduced below 300 K, the off-current drops to undetectable levels by 150 K, as the unintentional carriers (due to slight doping from air exposure) freeze out.

Over the moderate temperature range of 300 K to ~ 200 K, the mobility as inferred above at fixed small V_D is found to depend steeply on temperature. A small representative set of this data is shown in Fig. 1, where μ is plotted vs. inverse temperature for $V_G = -30, -40,$ and -50 V, for the $L = 300$ nm, $w = 3$ μm device at constant source-drain electric field of 1.3×10^7 V/m.

These data are approximately equally consistent with the three models mentioned above: simple Arrhenius behavior (the dashed line) with an activation energy ~ 100 meV; VRH

for a 2-D system (dotted line), of the form $\mu = \mu_0 \exp(-(T_0/T)^{1/3})$, where μ_0 and T_0 are fit parameters; and finally the more sophisticated percolative VRH theory (solid lines) developed by Vissenberg *et al*[7, 21]. The Vissenberg model's underlying assumptions include an exponential density of (localized) states (DOLS), $\nu(\epsilon) \sim \exp(\epsilon/k_B T_0)$, with transport of carriers dictated by percolative hopping. Since the gate voltage controls the Fermi level in the channel, and hence the occupation of the localized states, one finds that transport in the channel is strongly affected by V_G . Relevant fit parameters [7, 21] are: T_0 , describing the energy dependence of the DOLS; a prefactor σ_0 with units of conductivity; and α , an effective overlap parameter for hopping. Values used in the fits shown are $\sigma_0 = 7 \times 10^5$ S, $T_0 = 418$ K, $\alpha = 4.35 \times 10^9$ m⁻¹, consistent with those seen by other investigators in P3HT[21].

As temperatures are lowered from 200 K down to 10 K, over a broad range of source-drain and gate voltages, I_D evolves from approximately linear to a strongly nonlinear (superquadratic) dependence on V_D . An example of this evolution is shown in Fig. 2 for the $L = 3$ μm , $w = 30$ μm device, comparing data at 300 K and 70 K. We note that, at the lowest temperatures, smaller devices transport current *more easily* (larger currents at smaller gate voltages for a fixed V_D/L) than larger devices, as we will discuss later.

Analysis below shows that the nonlinear IV characteristics are described well by a model incorporating space-charge limited currents, modified by a Poole-Frenkel-like exponential dependence of effective mobility on square root of the local electric field (SCLPF). This conduction mechanism has been seen repeatedly in *two*-terminal devices[22, 23]. Room temperature experiments[25] on P3HT FETs with 70 nm channel lengths also show indications of SCL currents. We find that within this model, the temperature and gate voltage dependence of the data support a strongly energy dependent DOLS such as that in the Vissenberg picture. Other models may be possible, but they are constrained by the dependences presented below.

Charge transport in a device is space charge limited if the injected carriers significantly alter the local electric field from the average field imposed by the electrode potentials, and correspondingly limit the current. If, instead, the bottleneck in charge transport is injection at the contacts, a device is said to be contact limited, and is expected to exhibit Ohmic behavior at low source-drain fields. In principle, modeling our devices requires the full solution of the steady state charge and electric field profile in a three-terminal accumulation

mode transistor, including field- and temperature dependent effective mobility, and field- and temperature dependent contact properties. This general problem is very complex[26]; here we consider a simpler model and compare with the transport data.

In a system that is not contact limited, when the effective mobility varies as a function of electric field F , the space-charge limited current in a *two-terminal* device (a 1d model) is determined by the numerical solution of

$$\begin{aligned} J &= p(x)e\mu(F(x))F(x), \\ \frac{\kappa\epsilon_0}{e} \frac{dF}{dx} &= p(x), \end{aligned} \quad (1)$$

where $p(x)$ is the local hole density, $\int_0^L F(x)dx = V$, and the appropriate boundary condition on $F(x=0)$. For approximately Ohmic contacts, $F(x=0) \approx 0$.

We note that the case of an effective mobility that varies as

$$\mu(F) = \mu_0 \exp(\gamma\sqrt{F}) \quad (2)$$

and Ohmic contacts has been solved[27], and that the exact numerical solution is very well approximated by:

$$I \approx \frac{9}{8}\kappa\epsilon_0\mu_0 \left(\frac{V}{L}\right)^2 \frac{A}{L} \exp\left[0.9\gamma\left(\frac{V}{L}\right)^{1/2}\right]. \quad (3)$$

Here A is the device cross-sectional area, and L is the interelectrode distance. In our geometry L is the channel length, A is an effective cross-sectional area for the device (proportional to channel width), and κ is the relative dielectric constant of the semiconductor (chosen to be 3 in our analysis). The appearance of V/L in this equation does not imply that the electric field is constant over the device length. Rather, Eq. 3 suggests a means of plotting IV data to quickly ascertain consistency with the detailed numerical solution to the two-terminal SCLPF problem.

Note that μ_0 can depend on temperature; in a picture of hopping it should be proportional to the effective DOLS at the injecting contact. The dependence of mobility on $\exp(\sqrt{F})$ has long been seen in semiconducting and conducting polymers[28], and is associated with the charge carriers and disorder in these materials[4, 22, 29, 30]. The numerical solution of Ref. [27] (approximated by Eq. 3) should be valid as long as the functional form of the field-dependent mobility remains $\exp(\sqrt{F})$.

This equation is derived[23, 27] assuming that the charge distribution is determined by source-drain electrostatics only. The electric field from the gate certainly plays a nontrivial

role in our devices, clearly affecting charge injection, and allowing the formation of a channel at higher temperatures (since any charge present in the channel below dopant freeze-out has to be injected from the source and drain). For simplicity, however, in this model we will assume that the gate dependence will manifest itself through μ_0 , and that for fixed gate voltage we may treat the source-drain conductance like a two-terminal device.

Figure 3a shows a representative log-log plot of I_D vs. V_D for one sample with $L = 500$ nm and $V_G = -75$ V, for several temperatures. The solid lines are the numerical solution to Eq. 1, with parameters $A\mu_0$ and γ chosen at each temperature to give the best fit. The numerical solution is virtually indistinguishable from the analytic form of Eq. 3. Data on this and other samples for different gate voltages are qualitatively similar, with very good agreement between the numerical solution of the SCLPF model and the data. Fig. 3b shows the same data and fits replotted as suggested by Eq. (3). The quality of this agreement between the SCLPF model and the data in several devices over a broad range of T , V_G , and V_D/L is striking. Clearly for a given (large) V_G and (low) T , $I_D \sim V_D^2 \exp(\sqrt{V_D})$. Alternate explanations of the nonlinear conduction are strongly constrained by this dependence. The temperature and gate voltage range over which this form of source-drain nonlinearity occurs varies systematically with sample size, as described below.

A. Contact effects

One must consider whether the nonlinear $I_D - V_D$ characteristics result from nonlinear contact resistances as the temperature is decreased. For several reasons, discussed below, we do not believe this to be the case.

First we consider directly inferring the contact and channel resistances (R_s and R_{ch} , respectively) in the linear regime, and examining the temperature variation of their relative contributions. For a series of devices with fixed width, these resistances are calculated as follows[13, 14, 15, 16]: At a given T , the total resistance, $R_{on} \equiv \partial I_D / \partial V_D$, is calculated for each device at a small V_D and is plotted as a function of L for each gate voltage. The channel resistance per unit length, R_{ch}/L , at a given T and V_G is the slope ($\partial R_{on} / \partial L$) of such a graph, and the intercept (R_{on} extrapolated to $L = 0$) gives the parasitic series resistance, R_s .

For a fixed-aspect-ratio series of devices, one may follow an analogous procedure. The

total source-drain resistance $R_{\text{on}} = (L/w)R_{\square} + R_{\text{s}}$, where R_{\square} is the resistance per square of the channel. At a given T and V_G , $R_{\text{on}} \times w$ is plotted versus L for the series of devices. The slope of such a graph gives R_{\square} , and the intercept gives the total parasitic contact resistivity, $R_{\text{s}} \times w$. This analysis is shown in the fixed-aspect-ratio devices in Fig. 4 at room temperature for several gate voltages. For our geometry of $w/L = 10$, the inset shows the inferred $R_{\text{s}}/R_{\text{ch}}$ as a function of V_G , for a device with $L = 1 \mu\text{m}$. *Our series of fixed-aspect-ratio devices is clearly channel-limited at room temperature.*

This analysis may be repeated at different temperatures to examine the evolution of R_{s} and R_{ch} . We find that the nonlinear conduction at large average source-drain fields shown in the previous section makes this difficult to measure over a broad temperature range in the fixed-aspect-ratio device series. However, the fixed-width devices with longer channel lengths are well-suited to this approach down to 100 K. Figure 5 shows $R_{\text{s}}/R_{\text{ch}}$ as a function of temperature for the $L = 5 \mu\text{m}$ device from the $w = 100 \mu\text{m}$ series. Near room temperature, $R_{\text{s}} > R_{\text{ch}}$ for this device. As T decreases, while both R_{s} and R_{ch} increase significantly, R_{s} falls below R_{ch} near 100 K. The results of this experiment and others to be published elsewhere[24] demonstrate that the contact contributions become *less* important at low temperatures. This strongly suggests that the nonlinearities in the $I_D - V_D$ curves of short channel length devices observed at lower temperatures are unlikely to be contact effects.

Furthermore, the trends in transport with sample dimensions also support this conclusion. We find at low temperatures that the smallest devices actually transport charge considerably *better* than larger devices. For example, at 50 K for fixed V_D/L , the fixed-aspect-ratio $L = 300 \text{ nm}$ device exhibits measurable conduction for gate voltages as small as -25 V, while the $L = 3 \mu\text{m}$ device requires $V_G = -45 \text{ V}$. This trend is the *opposite* of what one would expect for contact-limited conduction[11]. Since w/L is held constant in this set of devices, shorter channel devices have significantly smaller contact areas as well, further emphasizing this point. The data are, however, consistent with the suggestion of space charge effects seen in 70 nm channel length P3HT FETs[25]. Finally, the voltage and temperature dependence of the data in Fig. 3 is not consistent with the forms for either classical Schottky contacts or Fowler-Nordheim emission. Detailed theory[31] and experiments[32] on injection into disordered polymer semiconductors show that injection efficiency can actually *improve* as temperature is decreased, consistent with our contact resistance data described above.

Coupled with the size dependence, this supports the idea that low temperature transport in our devices is *bulk* limited rather than contact limited.

B. Physical significance of fit parameters

Continuing within the SCLPF model and our analysis of the fixed-aspect-ratio devices, we note that, for identical effective mobilities and γ parameters, Eq. 3 implies that two samples with the same aspect ratio, thickness, and average source-drain field should give the same currents, independent of channel length, even deep in the nonlinear regime. Device-to-device variability in the effective mobility and γ , presumably due to differences in P3HT thickness and microstructure, make this challenging to check directly in our devices. For reasonable values of γ and V_D/L , a 10% variation in γ would lead to more than a factor of 2 variation in predicted current at low temperatures because of the exponential dependence in Eq. 3. However, if one fixes V_D/L and V_G , and normalizes measured currents by room temperature mobilities, one does indeed find scaling. For example, the $L = 500$ nm and $L = 1$ μm currents in the nonlinear regime normalized this way agree well all the way down to 10 K.

Within this model, the parameter γ should depend only on the hopping mechanism (*e.g.* thermal activation) and the nature of the localized states. We therefore expect γ to be independent of gate voltage for a given sample, and this is indeed seen in the inset to Fig. 6. At high temperatures ($T > 50$ K), the data for all gate voltages and all samples look roughly linear in $1/T$, consistent with thermally activated hopping. The magnitude of the slope of γ vs. $1/T$ is approximately $0.12 \text{ K(m/V)}^{1/2}$. This is consistent in magnitude with coefficients found in other semiconducting polymers such as poly(phenylene vinylene)[22]. However, γ vs. $1/T$ deviates significantly from a straight line at lower temperatures for all samples. This is consistent with a crossover from thermally activated hopping to a much less steep temperature dependence. A natural candidate is field enhanced tunneling between the localized states.

We now consider the gate and temperature dependence of the parameter $A\mu_0$ found by the numerical analysis above. The effective cross-section for current flow, A , is assumed to be temperature and gate voltage independent for each sample. In the linear regime at moderate temperatures it is known that the mobility inferred from the transconductance is gate voltage dependent, as seen in Fig. 1. This dependence on V_G continues in the apparent

SCLPF regime, as shown in Fig. 7a on an $L = 300$ nm device. The amount of variation of μ_0 with V_G , roughly a 5% increase of μ_0 per volt of V_G for this sample, shows no strong trend with temperature. The magnitude of this variation of mobility with V_G is consistent with that seen at higher temperatures in Fig. 1 for this sample. This exponential dependence of μ_0 on V_G is seen throughout the apparent SCLPF regime. As in the linear regime of an accumulation FET, gate voltage modulation of the conduction is *unipolar*: higher currents result only when V_G is made more negative.

The temperature dependence of μ_0 is also very strong, as shown in Fig. 7b for the same 300 nm channel sample at five gate voltages. The variation of $\mu_0(T)$ shown is much closer to an exponential in T to some slightly sublinear power rather than an Arrhenius or VRH form. This strong temperature dependence of μ_0 holds for all samples in the apparent SCLPF regime.

The strongly energy dependent DOLS employed in, for example, the Vissenberg model offers a natural explanation for these steep dependences of μ_0 on V_G and T . In the absence of any gate effect, the *effective* density of localized states available for hopping transport at some temperature T is given by $\nu(\epsilon \approx k_B T)$ where energy is measured from the band edge. An exponential DOLS of the Vissenberg model would then lead to an exponential dependence of μ_0 on T . Gate voltage dependence in this case comes from electrostatic modulation of the Fermi level in this rapidly varying DOLS. It is difficult to understand otherwise how an exponential dependence of the prefactor on T or V_G could arise. Deriving a quantitative relationship between V_G and the local Fermi level would require solving the full electrostatic problem of SCPLF conduction in the presence of the transverse gate field.

One can consider whether the proposed SCLPF conduction is a *bulk* process or one dominated by conduction in the thin channel layer active in standard FET operation. For the SCLPF mobility parameter μ_0 to coincide with the zero field mobility found at high temperatures in the linear regime, an effective cross-sectional area A considerably larger than $w \times$ a few nanometers is required. This is also true for the data of Ref. [25], in which a considerably different device geometry was used, if analyzed using the SCLPF model. However, the model of Eqs. (1),(2) does not account for the presence of a gate electrode or complicated source and drain geometries, and full computational modeling in this regime may be required to quantitatively account for this. One test for bulk vs. channel conduction would be to search for a correlation between P3HT thickness and currents in the apparent

SCL regime. This investigation is ongoing.

V. CONCLUSIONS

For a series of field effect devices with channel lengths ranging from 3 μm to 200 nm, we find gate modulated nonlinear conduction at low temperatures and high average source-drain electric fields. Analysis of channel and contact resistances as a function of temperature, and the dependence of conduction on sample size at low temperatures support the conclusion that this nonlinearity is unlikely to be a contact effect. We find that the data are well described by a model of gate modulated space-charge limited currents with Poole-Frenkel-like behavior of mobility. Within this model, the V_G and T dependence of the mobility prefactor is consistent with a very strongly energy dependent density of localized states. Finally, the temperature dependence of the Poole-Frenkel-like term within this model suggests a crossover from thermal hopping to quantum tunneling at low temperatures. Further studies of the field effect electrostatics problem, the metal-semiconductor contacts, and the low temperature nonthermal hopping process should lead to increased understanding of the conduction processes at work in these materials.

VI. ACKNOWLEDGMENT

The authors gratefully acknowledge the support of the Robert A. Welch Foundation.

FIG. 1: Mobility vs. T as computed from transconductance for three gate voltages, for a device with $L = 300$ nm from room temperature down to 200 K. Lines are fits to various models of hopping transport described in the text. Inset: cross-section of device showing bottom contact configuration and definition of channel length, L .

FIG. 2: I_D vs. V_D for the $L = 3 \mu\text{m}$, $w = 30 \mu\text{m}$ device, at 300 K (nearly linear, top) and 70 K (highly nonlinear, bottom). Curves from the top down correspond to V_G values from -95 V to -30 V in intervals of 5 V.

FIG. 3: (a) Log-Log plot of I_D vs. V_D for a device with $L = 500$ nm at $V_G = -75$ V. Solid lines indicate a numerical solution assuming space-charge limited conduction with a Poole-Frenkel-like field dependence of the mobility. (b) Plot of $\ln(I_D/V_D^2)$ vs. $\sqrt{V_D}$, as suggested by Eq. 3. Solid lines are fits to a linear dependence on $\sqrt{V_D}$.

FIG. 4: Plot of $R_{\text{on}} \times w$ vs. L for the fixed-aspect-ratio device series in the linear regime at 300 K for several gate voltages. Slopes of the linear fits correspond to R_{\square} of the channel, while intercepts correspond to the parasitic contact resistivity, $R_s w$. Inset: the ratio R_s/R_{ch} for the $L = 1 \mu\text{m}$, $w = 10 \mu\text{m}$ device. Clearly this device is *not* contact limited at room temperature.

FIG. 5: R_s/R_{ch} as a function of temperature as determined for the $w = 100 \mu\text{m}$, $L = 5 \mu\text{m}$ member of the fixed-width set of devices. Since this ratio decreases as T is lowered, contacts actually *improve* relative to the channel at low temperatures. This interesting result will be discussed more fully elsewhere[24].

FIG. 6: Inset: Plot of the parameter γ vs. V_G for the 500 nm sample of Fig. 3 at various temperatures ((top-to-bottom) 10 K, 30 K, 50 K, 70 K, 90 K, 120 K, 150 K, 180 K, 210 K) showing that γ is roughly gate voltage independent. Main figure: Plot of γ vs. $1/T$ for several samples, with γ averaged over gate voltages for each sample. Error bars are standard deviation. At high temperatures γ is expected to vary linearly in $1/T$, and all samples show a similar slope, $\gamma \times T \approx 0.12 \text{ (m/V)}^{1/2}$. Within this model, saturation of γ at low temperatures would indicate a crossover from thermal to nonthermal hopping transport at low temperatures.

FIG. 7: Assuming a fixed effective area $A = 3 \times 10^{-13} \text{ m}^2$, (a) Plot of the parameter μ_0 from plots like Fig. 3 vs. V_G for the 300 nm sample, from 210 K down to 10 K. (b) Plot of μ_0 vs. T for the same sample, for 5 different gate voltages. Note that μ_0 depends nearly exponentially on both temperature and gate voltage.

-
- [1] C.D. Dimitrakopoulos and D.J. Mascaró. IBM J. Res. Dev. **45** 11 (2001).
- [2] Z. Bao, J.A. Rogers, and H.E. Katz. J. Mat. Chem. **9** 1895 (1999).
- [3] H. Böttger and V.V. Bryskin, *Hopping Conduction in Solids* (Akademie-Verlag, Berlin, 1985).
- [4] P.E. Parris, V.M. Kenkre, and D.H. Dunlap. Phys. Rev. Lett. **87** 126601 (2001).
- [5] A.R. Brown, C.P. Jarrett, D.M. de Leeuw, and M. Matters. Synth. Met. **88** 37 (1997).
- [6] A.N. Aleshin, H. Sandberg and H. Stubb. Synth. Met. **121**, 1449 (2001).
- [7] M.C.J.M. Vissenberg and M. Matters. Phys. Rev. B **57** 12964 (1998).
- [8] C.D. Dimitrakopoulos, S. Purushothaman, J. Kymissis, A. Callegari, and J.M. Shaw. Science **283** 822 (1999).
- [9] G. Horowitz, R. Hajlaoui, D. Fichou, and A. El Kassmi. J. Appl. Phys. **85**, 3202 (1999).
- [10] K. Seshadri and C.D. Frisbie. Appl. Phys. Lett. **78**, 993 (2001).
- [11] R.A. Street and A. Salleo. Appl. Phys. Lett. **81**, 2887 (2002).
- [12] L. Bürgi, H. Sirringhaus, and R.H. Friend. Appl. Phys. Lett. **80**, 2913 (2002).
- [13] H. Klauk *et al.* Sol.-State Elect. **47**, 297 (2003).
- [14] P.V. Necludiov, M.S. Shur, D.J. Gundlach, and T.N. Jackson. Sol.-State Elect. **47**, 259 (2003).
- [15] J. Zaumseil, K.W. Baldwin, and J.A. Rogers. J. Appl. Phys. **93**, 6117 (2003).
- [16] E.J. Meijer, G.H. Gelinck, E. van Veenendaal, B.-H. Huisman, D.M. de Leeuw, and T.M. Klapwijk. Appl. Phys. Lett. **82**, 4576 (2003).
- [17] Sigma-Aldrich Inc., St. Louis, MO, USA.
- [18] Z. Bao, A. Dodabalapur, and A.J. Lovinger. Appl. Phys. Lett. **69** 4108 (1996).
- [19] H. Sirringhaus, N. Tessler, and R.H. Friend. Science **280** 1741 (1998).
- [20] H. Sirringhaus *et al.* Nature **401** 685 (1999).
- [21] E.J. Meijer *et al.* Appl. Phys. Lett. **80** 3838 (2002).
- [22] P.W.M. Blom, M.J.M. de Jong, and M.G. van Munster. Phys. Rev. B **55** R656 (1997).
- [23] G.G. Malliaras, J.R. Salem, P.J. Brock, and C. Scott. Phys. Rev. B **58** R13411 (1998).
- [24] B.H. Hamadani and D. Natelson. Submitted.
- [25] M.D. Austin and S.Y. Chou. Appl. Phys. Lett. **81** 4431 (2002).
- [26] M.A. Alam, A. Dodabalapur, and M.R. Pinto. IEEE Trans. Elect. Dev. **44** 1332 (1997).
- [27] P.N. Murgatroyd. J. Phys. D **3** 151 (1970).

- [28] W.D. Gill. *J. Appl. Phys.* **43** 5033 (1972).
- [29] S.V. Novikov, D.H. Dunlap, V.M. Kenkre, P.E. Parris, and A.V. Vannikov. *Phys. Rev. Lett.* **81**, 4472 (1998).
- [30] S.V. Rakhmanova and E.M. Conwell. *Appl. Phys. Lett.* **76** 3822 (2000).
- [31] V.I. Arkhipov, E.V. Emelianova, Y.H. Tak, and H. Bässler. *J. Appl. Phys.* **84** 848 (1998).
- [32] T. van Woudenbergh, P.W.M. Blom, M.C.J.M. Vissenberg, and J.N. Huiberts. *Appl. Phys. Lett.* **79** 1697 (2001).

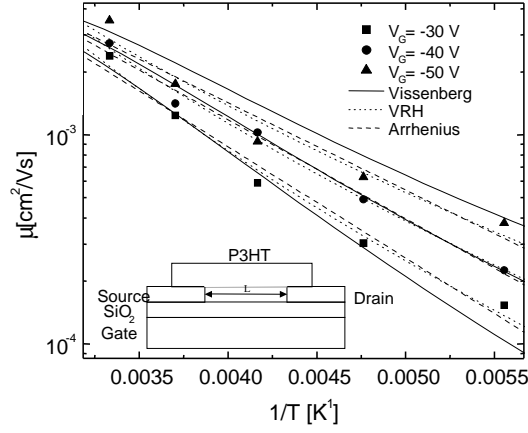


FIG. 1: of 7, B.H. Hamadani and D. Natelson “Gated nonlinear transport in organic polymer field effect transistors”, to appear in *J. Appl. Phys.*

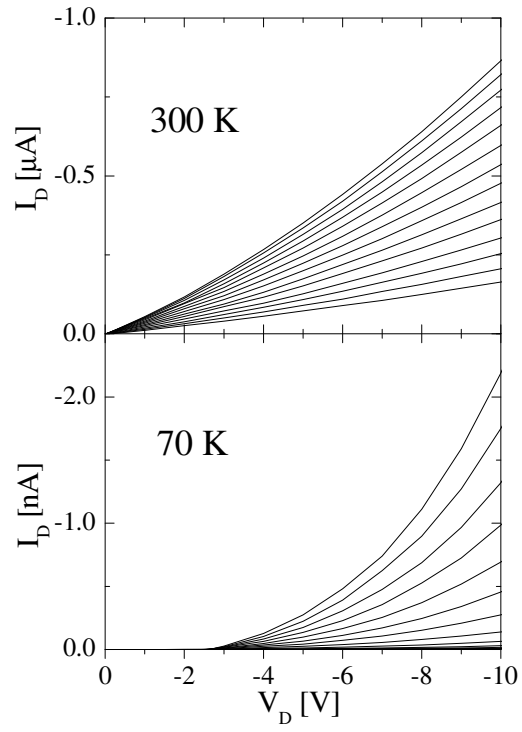


FIG. 2: of 7, B.H. Hamadani and D. Natelson “Gated nonlinear transport in organic polymer field effect transistors”, to appear in *J. Appl. Phys.*

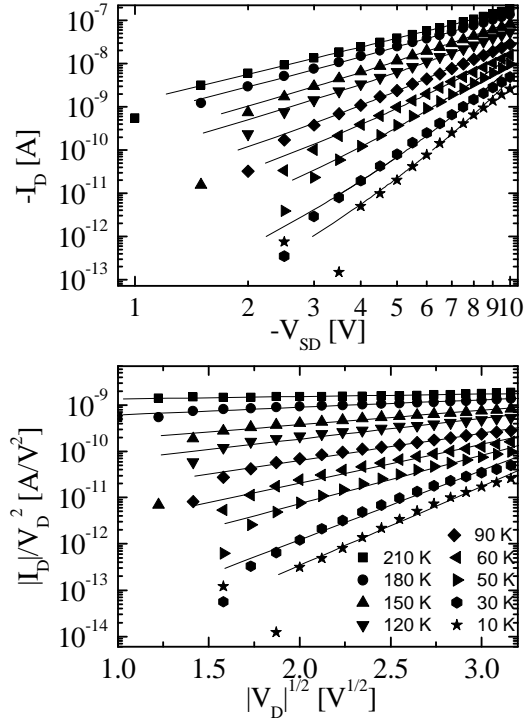


FIG. 3: of 7, B.H. Hamadani and D. Natelson “Gated nonlinear transport in organic polymer field effect transistors”, to appear in *J. Appl. Phys.*

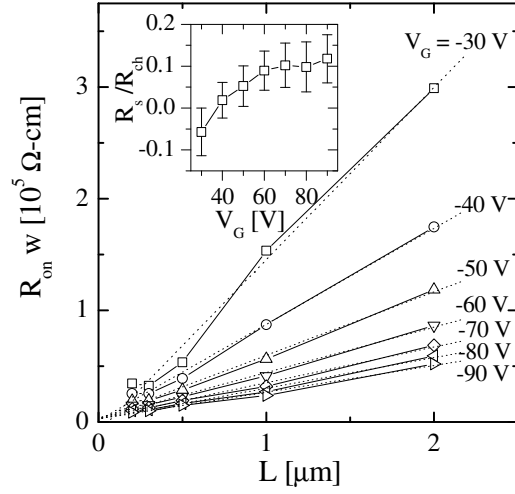


FIG. 4: of 7, B.H. Hamadani and D. Natelson “Gated nonlinear transport in organic polymer field effect transistors”, to appear in *J. Appl. Phys.*

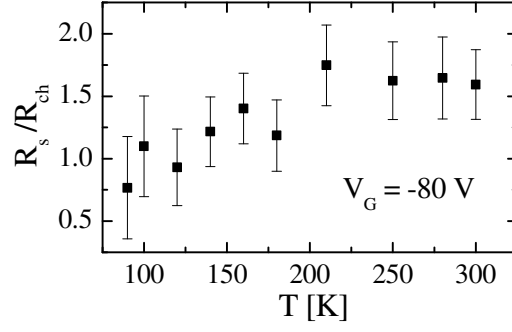


FIG. 5: of 7, B.H. Hamadani and D. Natelson “Gated nonlinear transport in organic polymer field effect transistors”, to appear in *J. Appl. Phys.*

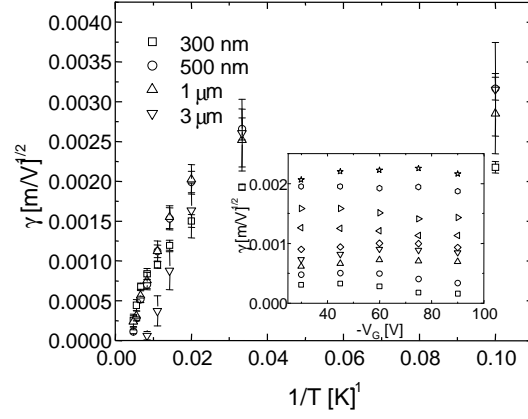


FIG. 6: of 7, B.H. Hamadani and D. Natelson “Gated nonlinear transport in organic polymer field effect transistors”, to appear in *J. Appl. Phys.*

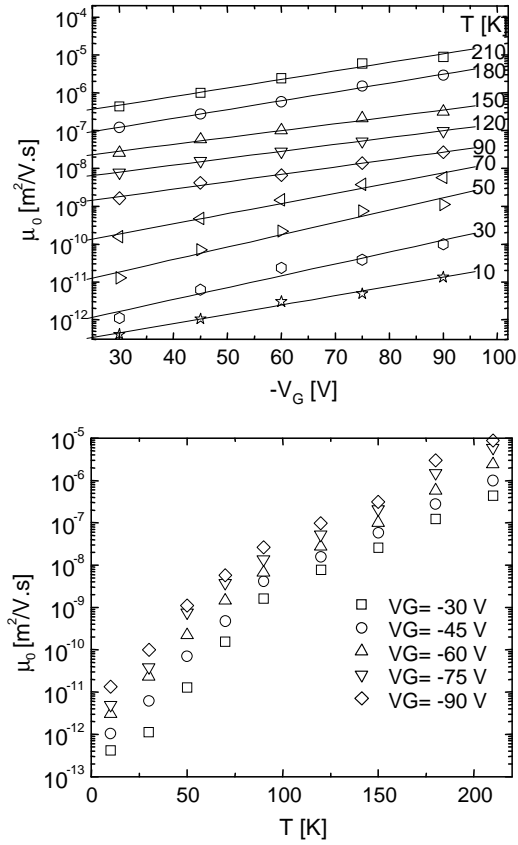


FIG. 7: of 7, B.H. Hamadani and D. Natelson “Gated nonlinear transport in organic polymer field effect transistors”, to appear in *J. Appl. Phys.*